Rapid Communications

Exact exchange-correlation kernels for optical spectra of model systems

M. T. Entwistle and R. W. Godby
Department of Physics, University of York, and European Theoretical Spectroscopy Facility, Heslington, York YO10 5DD, United Kingdom

(Received 13 December 2018; published 3 April 2019)

For two prototype systems, we calculate the exact exchange-correlation kernels $f_{xc}(x, x', \omega)$ of time-dependent density functional theory. f_{xc}, the key quantity for optical absorption spectra of electronic systems, is normally subject to uncontrolled approximation. We find that, up to the first excitation energy, the exact f_{xc} has weak frequency dependence and a simple, though nonlocal, spatial form. For higher excitations, the spatial behavior and frequency dependence become more complex. The accuracy of the underlying exchange-correlation potential is of crucial importance.

DOI: 10.1103/PhysRevB.99.161102

Time-dependent Kohn-Sham density functional theory [1,2] (TDDFT) is in principle an exact and efficient theory of the excited-state properties of many-electron systems, including a wide variety of important spectroscopies such as optical absorption spectra of molecules and solids. However, its application is restricted by the limitations of the available approximate functionals for electron exchange and correlation—in particular, the exchange-correlation kernel, f_{xc}, the functional derivative of the exchange-correlation potential with respect to the electron density. To assist the construction of more powerful approximations for f_{xc}, we calculate the *exact* f_{xc} for small prototype systems, and analyze its character, including key aspects in which it differs from the common approximations.

In the Runge-Gross formulation [1] of TDDFT the real system of interacting electrons is mapped onto an auxiliary system of noninteracting electrons moving in an effective local Kohn-Sham (KS) potential $v_{KS} = v_{ext} + v_H + v_{xc}$, with both systems having the same electron density n at all points in space and time. Many TDDFT calculations are done within the framework of linear response theory, which describes how a system responds upon application of a weak, time-dependent external perturbation. The induced density is described by the interacting density-response function, the functional derivative $\chi = \delta n/\delta v_{ext}$. χ is related to the noninteracting density-response function of the KS system, $\chi_0 = \delta n/\delta v_{KS}$, by the Dyson equation [3,4] $\chi = \chi_0 + \chi_0(u + f_{xc})\chi$, where u is the bare Coulomb interaction. χ_0 is to be obtained from a ground-state DFT calculation. χ can then be used to compute, for example, the optical absorption spectrum of the system,

$$\sigma(\omega) = -\frac{4\pi\omega}{c}\iint \mathrm{Im}[\chi(x, x', \omega)]xx'dx\,dx'. \qquad (1)$$

In practice, both v_{xc} and its functional derivative f_{xc} must be approximated. While there have been some successes, the commonly used adiabatic TDDFT functionals, such as the adiabatic local density approximation [5,6] (ALDA), often fail in extended systems. For example, the optical absorption spectra of many semiconductors and insulators are not even qualitatively described, with excitonic effects and many-electron excitations omitted [7,8], and the optical gap underestimated. Here, approximations for f_{xc} achieve little improvement over the random phase approximation (RPA), in which f_{xc} is neglected entirely [9]. Attempts to improve approximations for f_{xc} include exact-exchange methods [10–15], diagrammatic expansions using perturbative methods [16,17], and adding long-range contributions [18–21]. Another approach involves calculations of the homogeneous electron gas [22–26]. Kernels derived from the Bethe-Salpeter equation [27–31] have had some success, but require a relatively expensive many-body perturbation theory calculation as their input, and are outside the KS TDDFT framework.

There have been a limited number of studies conducted on analyzing the character of the exact f_{xc}, all of which focus on its frequency dependence. One approach has been to calculate the exact adiabatic f_{xc} for model systems [32], in order to investigate its performance upon application and deduce when memory effects become important. This approach has been used in simple Hubbard systems [33,34] and extended by analyzing additional properties, such as the frequency dependence of the full f_{xc} around double excitations. Other research has explored how this frequency dependence of f_{xc} turns the single-particle quantities of exact KS TDDFT into many-body excitations [35] and its behavior for long-range excitations has been analyzed in order to develop approximate kernels [36].

In this Rapid Communication, we explore the properties of exact xc kernels, including full spatial and frequency dependence, in order to inform the development of improved approximate functionals. We employ our iDEA code [37] which solves the many-electron Schrödinger equation exactly for small, one-dimensional prototype systems [38,39]. From the many-electron eigenstates of the system we calculate the exact χ using the Lehmann representation,

$$\chi(x, x', \omega) = \sum_m \left[\frac{\langle 0|\hat{n}(x)|m\rangle\langle m|\hat{n}(x')|0\rangle}{\omega - (E_m - E_0) + i\eta} + \mathrm{c.c.}(-\omega)\right], \qquad (2)$$

where $|0\rangle$, E_0, $|m\rangle$, and E_m are the ground state and its energy, and the mth excited state and its energy, respectively, $\hat{n}$ is the density operator in the Heisenberg picture, and η is a positive infinitesimal. χ has poles at the excitation energies of the

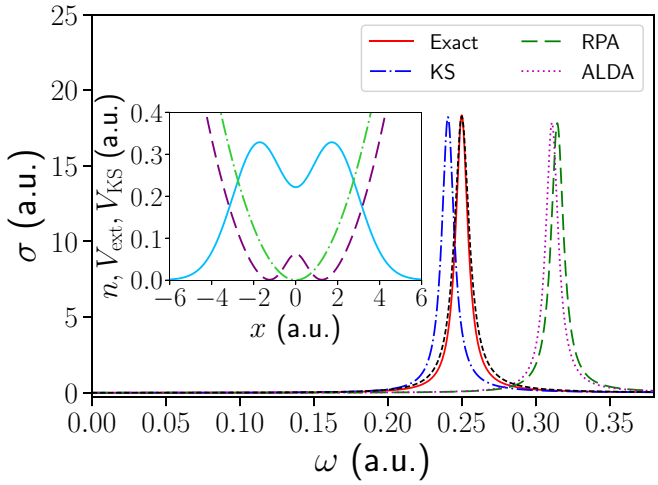

FIG. 1. Two interacting electrons in a harmonic potential. The inset shows the electron density (solid blue), along with the external (dotted-dashed green) and exact Kohn-Sham (dashed purple) potentials. In the main panel, the absorption spectra (detailing the first excitation) of the exact and Kohn-Sham systems, along with the RPA and ALDA approximations. We check that the calculated f_{xc} is correct by solving the Dyson equation and comparing the resultant absorption spectrum (short-dashed black) with the exact.

system, $E_m - E_0$. It is convenient to calculate $\mathrm{Im}(\chi)$, with $\mathrm{Re}(\chi)$ following from the Kramers-Kronig relations [40,41]. As is customary, we replace η with a small positive number, to broaden the absorption peaks for ease of viewing.

We then determine the exact KS potential through our reverse-engineering algorithm [42]. From the exact KS orbitals, we calculate the exact noninteracting density-response function,

$$\chi_0(x,x',\omega) = \sum_{i,j}(f_i - f_j)\frac{\phi_i^*(x)\phi_j(x)\phi_j^*(x')\phi_i(x')}{\omega - (\varepsilon_j - \varepsilon_i) + i\eta}, \qquad (3)$$

where the ϕ_i and ε_i are the exact solutions to the Kohn-Sham equations of ground-state DFT, and f_i is the Fermi occupation (0 or 1) of ϕ_i.

The Dyson equation may be manipulated into an expression for f_{xc},

$$f_{\mathrm{xc}} = \chi_0^{-1} - \chi^{-1} - u, \qquad (4)$$

but the inverses of χ and χ_0 are not well defined. For instance, a spatially uniform perturbation of any angular frequency induces no change in density, so both χ and χ_0 have a zero eigenvalue and therefore a zero determinant. To overcome this, we find a pseudoinverse of χ using truncated singular-value decomposition, discarding those eigenvectors with eigenvalues smallest in magnitude, which we term the eigenvalue cutoff. This procedure is repeated for χ_0, discarding the same number of eigenvectors. From the modified response functions a kernel f_{xc} is now well defined. We confirm the validity of this procedure by verifying that the calculated f_{xc}, together with the unmodified χ_0, closely reproduces the unmodified χ via the Dyson equation. Additionally, we ensure that the zero-force sum rule is obeyed—a well-known property of the exact f_{xc} [43].

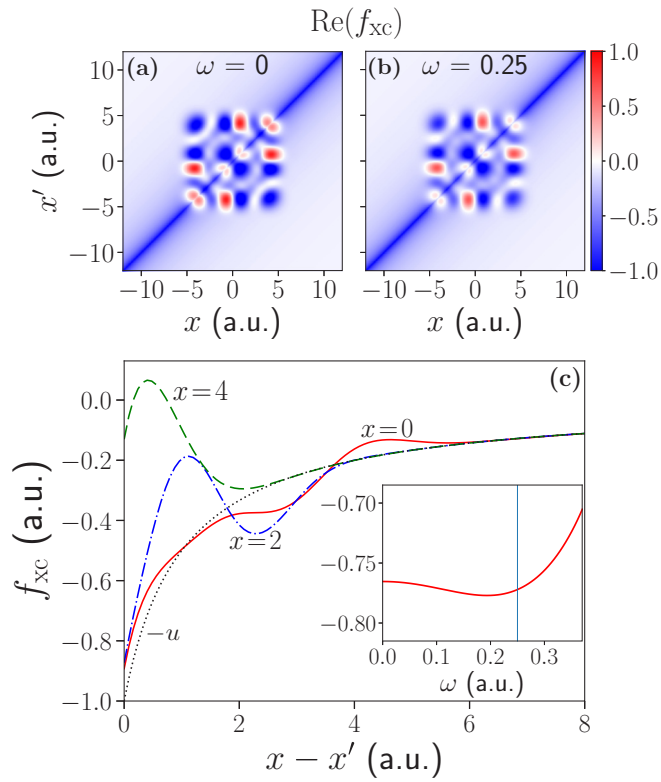

FIG. 2. The real part of the exact f_{xc} of the harmonic well system: (a) in the adiabatic limit ($\omega = 0$), and (b) at the first excitation ($\omega = 0.25$). (c) f_{xc} has a rather simple nonlocal dependence, which is similar to the negative of the Coulomb interaction u. Here we focus on f_{xc} at $\omega = 0.25$. Inset: We observe f_{xc} to have strikingly weak ω dependence up to the first excitation (vertical line). We illustrate this by plotting its value (solid red) at a point along the main diagonal ($x = x'$) which corresponds to the peak in electron density in the inset of Fig. 1 ($x = 1.7$ a.u.).

We begin by considering a system of two interacting electrons confined to a harmonic well potential ($\omega_0 = 0.25$ a.u.), where ω_0 is the angular frequency of the well (inset of Fig. 1). We compute the exact optical absorption spectrum of the system [44], with the first excitation at $\omega = \omega_0$ (Fig. 1). Additionally, we compute the absorption spectrum of the exact Kohn-Sham system, in which the absorption frequency is slightly too low ($\approx$0.01 a.u.). We also calculate the RPA and ALDA absorption spectra, in which the RPA and ALDA [45] kernels are combined with the *exact* χ_0. This last point provides a strong reminder of the challenge of f_{xc}: starting from the exact Kohn-Sham orbitals, a much better absorption peak is obtained by ignoring the induced changes in the Hartree and xc potentials (χ_0) than by accounting for the first exactly and either neglecting (RPA) or approximating (ALDA) the second. This highlights the importance of obtaining a good approximation to the ground-state xc potential v_{xc}, which leads to χ_0.

We now turn to the spatial characteristics of f_{xc} (Fig. 2). Typically, several different choices of the eigenvalue cutoff yield kernels f_{xc} with varying degrees of spatial structure, all of which essentially yield the correct χ from the exact χ_0 as set out above. Of these, we select the eigenvalue cutoff

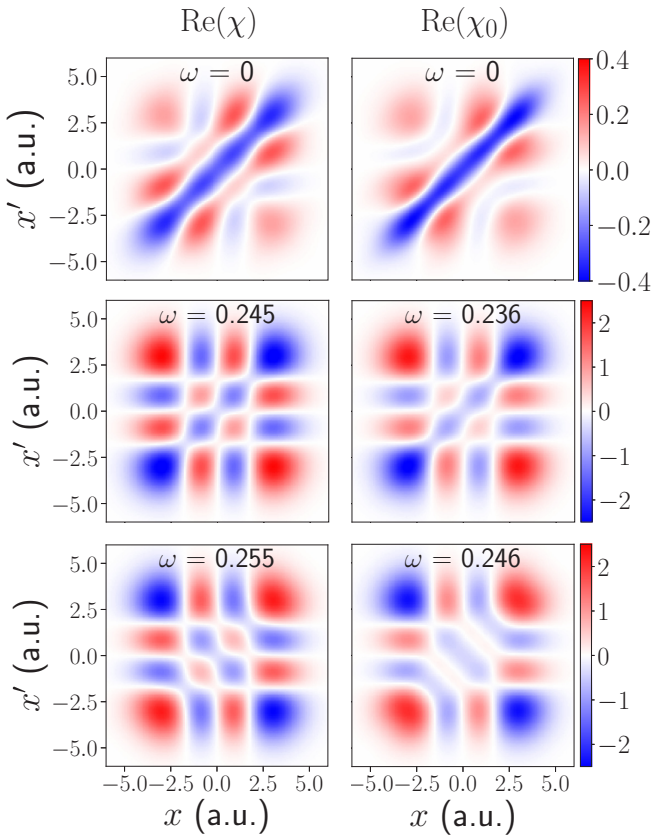

FIG. 3. The exact χ and χ_0 in the harmonic well system: Left: $\mathrm{Re}(\chi)$ at $\omega = 0$ and on either side of the transition at 0.250. Right: $\mathrm{Re}(\chi_0)$ at $\omega = 0$ and on either side of the transition at 0.241. $\mathrm{Re}(\chi)$ and $\mathrm{Re}(\chi_0)$ exhibit remarkably similar spatial structure.

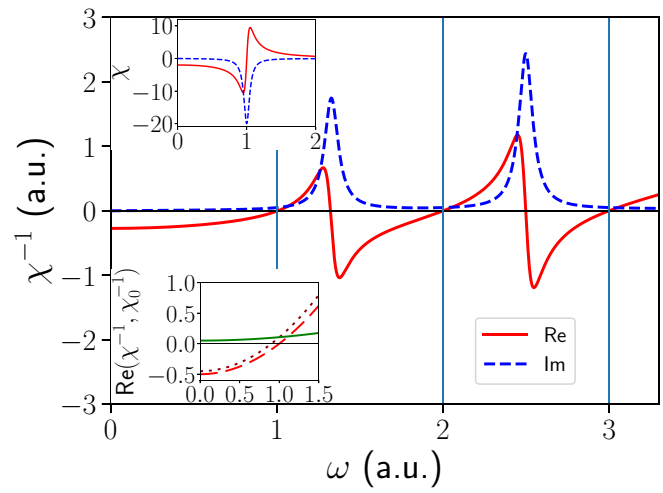

FIG. 4. The top inset shows χ for a simple model without spatial dependence and a single excitation at $\omega = 1$; the bottom inset shows the near cancellation (solid green) between $\mathrm{Re}(\chi^{-1})$ (dashed red) and $\mathrm{Re}(\chi_0^{-1})$ (dotted dark red), where χ_0 has an excitation at 0.9, causing f_{xc} to exhibit weak ω dependence. In the main panel, two further excitations at $\omega = 2$ and 3 have been included, to show that $\mathrm{Re}(\chi^{-1})$ passes through zero between excitations, which leads to a nonzero $\mathrm{Im}(f_{\mathrm{xc}})$, as does the corresponding feature in χ_0^{-1} (not shown).

with the largest magnitude, resulting in the smoothest possible spatial structure without detriment to the exact absorption spectrum (Fig. 1). We observe that while f_{xc} has real and imaginary parts (see later), the real part alone is sufficient to reproduce the position and weight of the first excitation ($\omega = \omega_0$). Figures 2(a) and 2(b) show $\mathrm{Re}(f_{\mathrm{xc}})$ at $\omega = 0$ and ω_0, respectively. The behavior of f_{xc} away from the diagonal, $x \neq x'$, represents the kernel's nonlocality, and it is evident that this is fairly simple in nature; analysis [Fig. 2(c)] shows it to be similar to the negative of the Coulomb interaction, with which it therefore tends to cancel in the expression for χ. The ω dependence of f_{xc} up to the first excitation is seen to be extremely weak, as observed in other model systems [33–35]. We analyze this more closely in the inset to Fig. 2(c).

To gain insight into these observations, we analyze the exact χ and χ_0. Figure 3 shows $\mathrm{Re}(\chi)$ and $\mathrm{Re}(\chi_0)$; up to the first excitation, these exhibit strong, but closely similar, ω dependence. The similarity arises in part from the exact many-electron wave function being well approximated by the exact Kohn-Sham wave function [46], which reflects the dominance of exchange (including self-interaction correction) in the harmonic potential system [47]. Therefore χ^{-1} and χ_0^{-1} largely cancel, so that f_{xc} is similar to $-u$, with weak ω dependence.

This can be demonstrated succinctly through a simple model, in which we take Eqs. (2) and (3), and replace the spatially dependent numerators (the oscillator strengths) with scalars. Specifically, we consider a system with a single excitation at $\omega = 1$, set the numerator equal to 1, and let $\eta = 0.05$ (top inset of Fig. 4). We do the same for the Kohn-Sham system, but choose the excitation to occur at $\omega = 0.9$. By taking their inverses, we calculate $\mathrm{Re}(\chi_0^{-1} - \chi^{-1})$, which is the ω-dependent part of $\mathrm{Re}(f_{\mathrm{xc}})$ in Eq. (4), and find this to be small in amplitude and have a fairly weak ω dependence up to the first excitations (bottom inset of Fig. 4). The inclusion of higher excitations, and taking the limit $\eta \to 0$, change little at these low frequencies.

Including higher excitations in the model χ causes $\mathrm{Re}(\chi)$ to pass through zero between excitations. At these points $\mathrm{Re}(\chi^{-1})$ also passes through zero, and $\mathrm{Im}(\chi^{-1})$ peaks sharply (Fig. 4). As $\mathrm{Im}(f_{\mathrm{xc}}) = \mathrm{Im}(\chi_0^{-1} - \chi^{-1})$, we find that the f_{xc} in our simple model only has an imaginary component when χ or χ_0 passes through zero between excitations, and hence is completely real up to the first excitations (as $\eta \to 0$). This supports our finding in the harmonic well system, in which $\mathrm{Im}(f_{\mathrm{xc}})$ was very small up to the first excitations, and $\mathrm{Re}(f_{\mathrm{xc}})$ was sufficient to reproduce the peak in the absorption spectrum.

We now consider a system whose absorption spectrum includes higher excitations—two interacting electrons in a softened atomiclike potential (top inset of Fig. 5). As in the harmonic well system, the absorption spectrum of the exact Kohn-Sham system is slightly too low for the first excitation (Fig. 5). Again, we find f_{xc} to be dominated by its real part and nearly ω independent, while exhibiting relatively simple spatial structure, up to and including the first excitation [Fig. 6(a)]. The second excitation does not appear in the absorption spectrum, and so we move to the third excitation, which is much smaller in amplitude than the first, and once more observe the peak in the Kohn-Sham system to be slightly

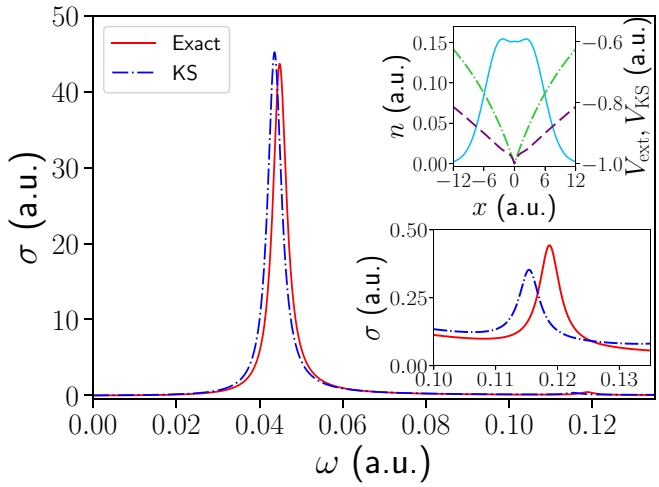

FIG. 5. Two interacting electrons in an atomiclike potential. The top inset shows the electron density (solid blue), along with the external (dotted-dashed green) and Kohn-Sham (dashed purple) potentials. In the main panel, the absorption spectra of the exact and Kohn-Sham systems; the bottom inset shows the third excitation (fourth in the KS system) in more detail, which is the next to appear after the first excitation.

below but still very close to the exact (bottom inset of Fig. 5). Again, the closeness between the two peaks arises from the strong similarity between χ and χ_0. In order to reproduce this excitation, a smaller eigenvalue cutoff is required, leading to higher spatial frequencies in f_{xc} [48] [Fig. 6(b)].

For the atomlike system, we have investigated the extent to which local kernel approximations for f_{xc} may be meaningful. As we have observed f_{xc} to largely cancel with u at low ω, we choose to focus on the Hartree exchange-correlation kernel $f_{\mathrm{Hxc}} = f_{\mathrm{xc}} + u$ which is more local. We incorporate the nonlocal parts of f_{Hxc} by projecting them onto a local kernel [49]. We find this largely corrects the difference $\chi_0 - \chi$, and hence the position of the peak in the absorption spectrum, for the first excitation, but fails to correct the height of the peak. Such a local kernel is completely inadequate to describe the third excitation.

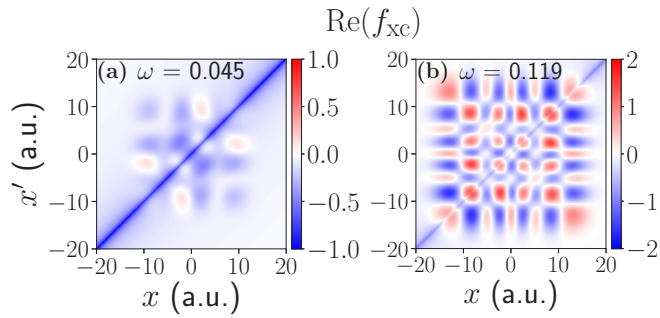

FIG. 6. The real part of the exact f_{xc} of the atomlike system: (a) at the first excitation ($\omega = 0.045$), and (b) at the third excitation ($\omega = 0.119$). As in the harmonic well system, we find f_{xc} to be nearly ω independent and exhibit a relatively simple spatial form up to the first excitation. However, a more complex spatial structure is needed to capture higher excitations.

In summary, we have calculated the exact $f_{\mathrm{xc}}(x, x', \omega)$ for two prototype systems. At low ω, we find the imaginary component of f_{xc} to be small, with the real part alone sufficient to reproduce the first excitation. Up to and including the first excitation, $\mathrm{Re}(f_{\mathrm{xc}})$ exhibits strikingly weak ω dependence, stemming from strong, but closely similar ω dependence between the interacting and noninteracting density-response functions, boding well for the applicability of adiabatic kernels. Additionally, $\mathrm{Re}(f_{\mathrm{xc}})$ here has a rather simple spatial form, which is similar to the negative of the Coulomb interaction u, indicating that approximations to f_{Hxc} may be more appropriate than those for f_{xc} alone. For higher excitations, f_{xc} exhibits both additional spatial structure and stronger ω dependence, indicating that more sophisticated approximations are needed. Throughout, the absorption spectrum of the exact Kohn-Sham system provides a very good starting point, signifying the crucial importance of an accurate approximation for the ground-state v_{xc}.

Data created during this research is available from the York Research Database [50].

We thank Phil Hasnip for helpful discussions.

[1] E. Runge and E. K. U. Gross, Phys. Rev. Lett. **52**, 997 (1984).
[2] E. K. U. Gross, J. F. Dobson, and M. Petersilka, Density Functional Theory of Time-Dependent Phenomena, in *Density Functional Theory II: Relativistic and Time Dependent Extensions*, edited by R. F. Nalewajski (Springer, Berlin/Heidelberg, 1996), pp. 81–172.
[3] Matrix multiplication for the spatially nonlocal quantities χ, χ_0, and f_{xc}, and ω dependence, are implied.
[4] M. Petersilka, U. J. Gossmann, and E. K. U. Gross, Phys. Rev. Lett. **76**, 1212 (1996).
[5] A. Zangwill and P. Soven, Phys. Rev. A **21**, 1561 (1980).
[6] E. K. U. Gross and W. Kohn, Phys. Rev. Lett. **55**, 2850 (1985).
[7] C. Jamorski, M. E. Casida, and D. R. Salahub, J. Chem. Phys. **104**, 5134 (1996).
[8] N. T. Maitra, F. Zhang, R. J. Cave, and K. Burke, J. Chem. Phys. **120**, 5932 (2004).
[9] V. I. Gavrilenko and F. Bechstedt, Phys. Rev. B **55**, 4343 (1997).
[10] Y.-H. Kim and A. Görling, Phys. Rev. Lett. **89**, 096402 (2002).
[11] Y.-H. Kim and A. Görling, Phys. Rev. B **66**, 035114 (2002).
[12] A. Görling, Phys. Rev. A **57**, 3433 (1998).
[13] M. Hellgren and U. von Barth, J. Chem. Phys. **131**, 044110 (2009).
[14] A. Ipatov, A. Heßelmann, and A. Görling, Int. J. Quantum Chem. **110**, 2202 (2010).
[15] A. Görling, Phys. Rev. Lett. **83**, 5459 (1999).
[16] I. V. Tokatly and O. Pankratov, Phys. Rev. Lett. **86**, 2078 (2001).
[17] I. V. Tokatly, R. Stubner, and O. Pankratov, Phys. Rev. B **65**, 113107 (2002).

[18] S. Botti, F. Sottile, N. Vast, V. Olevano, L. Reining, H.-C. Weissker, A. Rubio, G. Onida, R. Del Sole, and R. W. Godby, Phys. Rev. B **69**, 155112 (2004).
[19] S. Sharma, J. K. Dewhurst, A. Sanna, and E. K. U. Gross, Phys. Rev. Lett. **107**, 186401 (2011).
[20] P. E. Trevisanutto, A. Terentjevs, L. A. Constantin, V. Olevano, and F. D. Sala, Phys. Rev. B **87**, 205143 (2013).
[21] S. Rigamonti, S. Botti, V. Veniard, C. Draxl, L. Reining, and F. Sottile, Phys. Rev. Lett. **114**, 146402 (2015).
[22] V. U. Nazarov, I. V. Tokatly, S. Pittalis, and G. Vignale, Phys. Rev. B **81**, 245101 (2010).
[23] Z. Qian and G. Vignale, Phys. Rev. B **65**, 235121 (2002).
[24] C. F. Richardson and N. W. Ashcroft, Phys. Rev. B **50**, 8170 (1994).
[25] S. Conti, R. Nifosì, and M. P. Tosi, J. Phys.: Condens. Matter **9**, L475 (1997).
[26] M. Panholzer, M. Gatti, and L. Reining, Phys. Rev. Lett. **120**, 166402 (2018).
[27] G. Onida, L. Reining, and A. Rubio, Rev. Mod. Phys. **74**, 601 (2002).
[28] L. Reining, V. Olevano, A. Rubio, and G. Onida, Phys. Rev. Lett. **88**, 066404 (2002).
[29] F. Sottile, V. Olevano, and L. Reining, Phys. Rev. Lett. **91**, 056402 (2003).
[30] G. Adragna, R. Del Sole, and A. Marini, Phys. Rev. B **68**, 165108 (2003).
[31] A. Marini, R. Del Sole, and A. Rubio, Phys. Rev. Lett. **91**, 256402 (2003).
[32] M. Thiele and S. Kümmel, Phys. Rev. A **80**, 012514 (2009).
[33] F. Aryasetiawan and O. Gunnarsson, Phys. Rev. B **66**, 165119 (2002).
[34] D. J. Carrascal, J. Ferrer, N. Maitra, and K. Burke, Eur. Phys. J. B **91**, 142 (2018).
[35] M. Thiele and S. Kümmel, Phys. Rev. Lett. **112**, 083001 (2014).
[36] N. T. Maitra and D. G. Tempel, J. Chem. Phys. **125**, 184111 (2006).
[37] M. J. P. Hodgson, J. D. Ramsden, J. B. J. Chapman, P. Lillystone, and R. W. Godby, Phys. Rev. B **88**, 241102(R) (2013).
[38] We perform calculations for systems of two spinless electrons interacting via the appropriately softened Coulomb repulsion [51] $u(x,x') = (|x-x'|+1)^{-1}$, and work in Hartree atomic units: $m_e = \hbar = e = 4\pi\varepsilon_0 = 1$.
[39] See Supplemental Material at http://link.aps.org/supplemental/10.1103/PhysRevB.99.161102 for the parameters of the model systems, and details on our calculations to obtain converged results.
[40] D. Pines, *Elementary Excitations in Solids: Lectures on Phonons, Electrons, and Plasmons*, Lecture Notes and Supplements in Physics (W. A. Benjamin, New York, 1964).
[41] M. Marder, *Condensed Matter Physics* (Wiley, New York, 2010).
[42] J. D. Ramsden and R. W. Godby, Phys. Rev. Lett. **109**, 036402 (2012).
[43] See Supplemental Material at http://link.aps.org/supplemental/10.1103/PhysRevB.99.161102 for more details.
[44] For this harmonic well system, at the level of linear response theory, only one excitation appears in the absorption spectrum.
[45] M. T. Entwistle, M. Casula, and R. W. Godby, Phys. Rev. B **97**, 235143 (2018).
[46] We define this as a Slater determinant of the occupied KS orbitals.
[47] E. Richardson (private communication).
[48] As expected for higher energy excited states.
[49] We fold the nonlocal f_{Hxc} with an envelope function that suppresses the more distant nonlocal parts and projects the remainder onto the diagonal $x = x'$.
[50] M. T. Entwistle and R. W. Godby, Data related to "Exact exchange-correlation kernels for optical spectra of model systems", http://dx.doi.org/10.15124/56f576ee-b2de-4ca5-9251-831bfc3cae6f (2019).
[51] A. Gordon, R. Santra, and F. X. Kärtner, Phys. Rev. A **72**, 063411 (2005).